Available online at www.sciencedirect.com
ScienceDirect
Chaos, Solitons and Fractals 36 (2008) 772–780
CHAOS SOLITONS & FRACTALS
www.elsevier.com/locate/chaos

Stability analysis of the kicked harmonic oscillator's accelerator modes

G.A. Kells [a,*], J. Twamley [b], D.M. Heffernan [a]

[a] Department of Mathematical Physics, National University of Ireland, Maynooth, Ireland
[b] Centre for Quantum Computer Technology, Macquarie University, Sydney, New South Wales 2109, Australia

Accepted 3 July 2006

Communicated by Prof. El Naschie.

Abstract

We use the idea of primary ballistic trajectories to analyse the structure and derive the stability conditions of the 'accelerator modes' or 'ballistic channels' that exist in the kicked harmonic oscillator and kicked Harper models.

1. Introduction

The kicked harmonic oscillator (KHO) was originally proposed as a 2-dimensional model of charges moving in a homogeneous static magnetic field while under the influence of an orthogonal time-dependent electric field [1–5]. The model is fundamentally different from other widely studied kicked systems because the natural frequency of the unperturbed system does not depend on energy. It therefore cannot be described using the KAM theorem [6–8]. The quantized system has been proposed as a model for electronic transport in semiconductor super-lattices [9,10] and for atom optic modeling in ion-traps [11]. As we will see below, when a ratio of 1/4 exists between the kicking and oscillation frequencies the KHO can be related to the kicked Harper model (KHM). This is a generalisation of the *ordinary* Harper model [12] introduced to approximate electron dynamics confined to a 2-dimensional lattice while under the influence of a perpendicular magnetic field [13,14]. The primary goal of this article is to examine the stability properties of ballistic or accelerator channels that occur in these kicked systems for certain ranges of the perturbation strength. We will show that the largest channel is stable when the kicking strength μ is in the range

$$2m\pi < \mu < \sqrt{(2m\pi)^2 + 4}. \tag{1}$$

Additional information on the web map and on accelerator modes in general can be found in the articles [15–17].

* Corresponding author. Tel.: +353 1 708 3548; fax: +353 1 708 3967.
E-mail address: gkells@thphys.nuim.ie (G.A. Kells).

0960-0779/$ - see front matter
doi:10.1016/j.chaos.2006.07.017

2. Background

The Hamiltonian for the KHO may be written symmetrically in position q and momentum p as

$$\mathscr{H}(q,p,t) = \frac{\omega_0}{2}(p^2+q^2) + \frac{\mu}{k}\cos kq \sum_{n=-\infty}^{\infty} \delta(t-nT), \tag{2}$$

see [18] for the derivation. The first part is just the Hamiltonian of a free harmonic oscillator with a frequency of ω_0. The period of such an oscillator is thus $T_0 = 2\pi/\omega_0$. The frequency of the kicking pulse is given by $\omega = 2\pi/T$. We define the *frequency ratio* as $1/R = \omega_0/\omega = \omega_0 T/2\pi$. When the frequency ratio is 1/4 the motion of a particle initially at (q_0,p_0) may be written as the following iterative mapping

$$\begin{aligned} p_{n+1} &= -q_n, \\ q_{n+1} &= p_n + \mu\sin(kq_n), \end{aligned} \tag{3}$$

where it is assumed that (q_n,p_n) refers to the phase space configuration just before the $(n+1)$th kick. Setting $k = 1$ and iterating once more we obtain

$$\begin{aligned} p_{n+2} &= -p_n - \mu\sin(q_n), \\ q_{n+2} &= -q_n + \mu\sin(p_n + \mu\sin(q_n)). \end{aligned} \tag{4}$$

This map may be trivially linked to web map of the KHM by rotating the resulting configuration through π radians about phase plane origin. This gives

$$\begin{aligned} p' &= p + \mu\sin(q), \\ q' &= q - \mu\sin(p'), \end{aligned} \tag{5}$$

where we have set $(q_n,p_n) = (q,p)$ and $(q_{n+2},p_{n+2}) = (q',p')$. This corresponds to the symmetrical case of the KHM when $K = L = \mu$, see Fig. 1. The use of this related map makes the subsequent analysis a little easier.

Diffusion in the KHM and KHO is defined as the mean rate of energy growth of a large ensemble of initial configurations over a 'long' time. The energy of each configuration is calculated using the simple harmonic oscillator

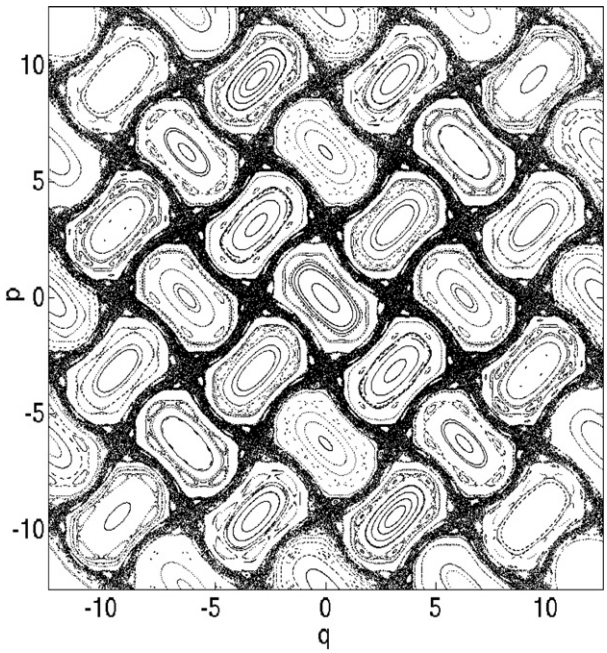

Fig. 1. Poincaré surface of section for the kicked Harper model with $k = 1$, $\mu = K = L = 1.5$. The mapping (5) is often called the web map for obvious reasons.

Hamiltonian, that is $E_n = \frac{\omega_0}{2}(q_n^2 + p_n^2)$. The rate of linear energy growth or diffusion over N iterations is then defined as $D(\mu) = (\langle E_N \rangle - \langle E_0 \rangle)/N$. Analysis in [14] calculates the rate of diffusion, when $k = 1$, to be

$$D(\mu) = \frac{1}{4}\mu^2[1 - 2J_0(\mu) - 2J_0^2(\mu)], \tag{6}$$

while that of [19–21] gives

$$D(\mu) = \frac{1}{4}\mu^2[1 - 2J_1^2(\mu) - 2J_2 + 2J_2^2(\mu) + 2J_3^2(\mu)]. \tag{7}$$

We compare these functions with the numerically calculated values of the diffusion coefficient in Fig. 2. The results show that while being an extremely good fit for most kicking strengths neither analysis accounts for the sharp spikes that occur when the kicking strength μ is just above a multiple of 2π. These spikes are the result of the accelerator or ballistic channels mentioned in the introduction. They are stable structures in the phase plane that are continually translated in the same direction under each operation of the map (5).

3. The primary ballistic trajectories

Careful examination of (5) allows us introduce the concept of a *primary trajectory* of a ballistic channel. Consider the case with $\mu = 2m\pi$ and $(q,p) = (Q,P) = (n_q\pi/2, n_p\pi/2)$ where n_p, n_q and m are all integers. After a little work the mapping can be written as

$$\begin{aligned} P' &= P + 2m\pi(-1)^{\frac{1}{2}(n_q-1)}\varepsilon(n_q), \\ Q' &= Q - 2m\pi(-1)^{\frac{1}{2}(n_p-1)}\varepsilon(n_p). \end{aligned} \tag{8}$$

where

$$\varepsilon(n) = 0 \quad n \text{ even}, \tag{9}$$

$$\varepsilon(n) = 1 \quad n \text{ odd}. \tag{10}$$

From this map we can discern eight distinct directions in the phase plane in which a particle is continually translated upon operation of the map. For example if we set $\mu = 2\pi$ and $(q,p) = (\pi/2, 3\pi/2)$ we see that subsequent values of p' and q' gain $+2$ π and therefore move in the direction $\hat{\imath} + \hat{\jmath}$ in the plane. Likewise a particle at $(q,p) = (3\pi/2, 3\pi/2)$ would move in the direction of $-\hat{\imath} + \hat{\jmath}$ and one at $(q,p) = (\pi, 5\pi/2)$ would move in the $-\hat{\imath}$ direction. We will define these paths as *primary trajectories* of the ballistic channels.

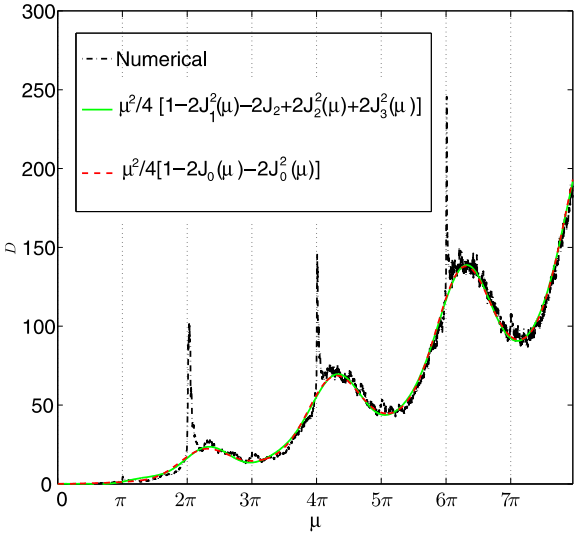

Fig. 2. $D - v - \mu$ for kicked harmonic oscillator with frequency ratio $1/R = 1/4$. The numerical calculation was performed by taking 2000 randomly distributed particles in the phase plane and evolving for 500 discrete time steps at different μ. Analytical estimates of the curve fail to account for the sharp spikes that occur around $\mu = 2m\pi$ for integer m.

Continuity of the kicking parameter μ and of the sin function in (5) dictates that particles in the vicinity of a primary trajectory should remain close for a number of iterations. To examine the stability of these surrounding trajectories it is therefore logical to analyse the mapping from the reference frame of a primary trajectory. To do this we set $\mathscr{P} = p - P$, $\mathscr{Q} = q - Q$ and simply subtract (8) from (5). If both n_p and n_q are odd one then obtains

$$\begin{aligned} \mathscr{P}' &= \mathscr{P} + (-1)^{\frac{1}{2}(n_q-1)}[\mu\cos(\mathscr{Q}) - 2m\pi], \\ \mathscr{Q}' &= \mathscr{Q} - (-1)^{\frac{1}{2}(n_p-1)}[\mu\cos(\mathscr{P}') - 2m\pi]. \end{aligned} \tag{11}$$

We show phase space diagrams for the above mapping for a number of different μ in Fig. 3. If n_p is odd and n_q is even one gets

$$\begin{aligned} \mathscr{P}' &= \mathscr{P} + (-1)^{\frac{1}{2}(n_q)}\mu\sin(\mathscr{Q}), \\ \mathscr{Q}' &= \mathscr{Q} - (-1)^{\frac{1}{2}(n_p-1)}[\mu\cos(\mathscr{P}') - 2m\pi], \end{aligned} \tag{12}$$

and if n_p is even and n_q is odd one gets

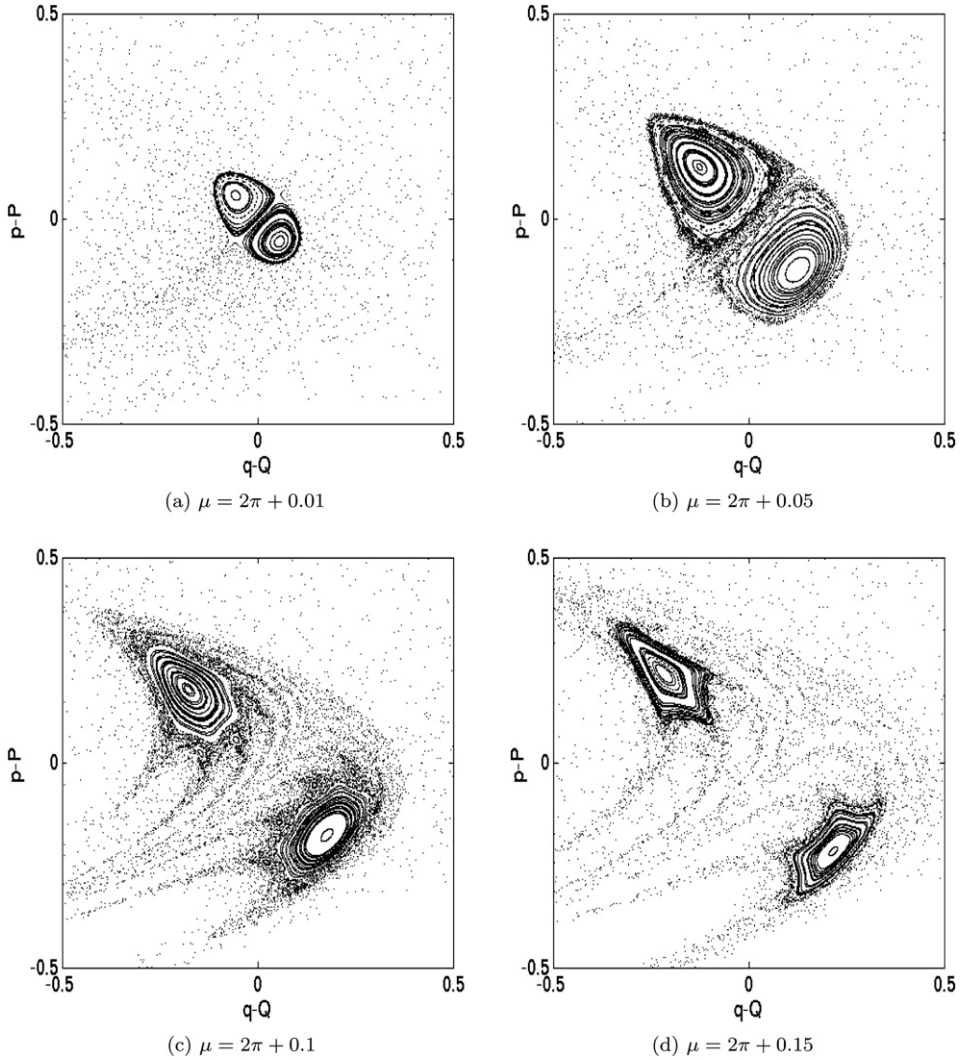

Fig. 3. Graphs showing structure of a ballistic island for various values of the kicking strength μ. These graphs are generated by operating on a group of randomly distributed points in the phase plane window $\mathscr{Q}, \mathscr{P} \in [-0.5, 0.5]$ with the map (11).

$$\begin{aligned}\mathscr{P}' &= \mathscr{P} + (-1)^{\frac{1}{2}(n_q-1)}[\mu\cos(\mathscr{Q}) - 2m\pi],\\ \mathscr{Q}' &= \mathscr{Q} - (-1)^{\frac{1}{2}(n_p)}\mu\sin(\mathscr{P}').\end{aligned} \tag{13}$$

Some examples of the stable structures generated by (12) are given in Fig. 4.

4. Stability analysis

We first deal with the diagonal ballistic channels of the type given in (11). Exact return points in these maps occur when $\mathscr{P}' = \mathscr{P}$ and $\mathscr{Q}' = \mathscr{Q}$. Solving for $\mathscr{P}$ and $\mathscr{Q}$ gives four points at $(\mathscr{Q}, \mathscr{P}) = (l_q, l_p) = (\pm l, \pm l)$ where $l = \cos^{-1}(2m\pi/\mu)$. It is immediately apparent that return points only exist if $\mu \geqslant 2m\pi$ (Fig. 5).

One can now calculate the Jacobian matrix

$$\mathbf{J} = \begin{pmatrix} \frac{\partial\mathscr{Q}'}{\partial\mathscr{Q}} & \frac{\partial\mathscr{Q}'}{\partial\mathscr{P}} \\ \frac{\partial\mathscr{P}'}{\partial\mathscr{Q}} & \frac{\partial\mathscr{P}'}{\partial\mathscr{P}} \end{pmatrix} = \begin{pmatrix} \frac{\partial\mathscr{Q}'}{\partial\mathscr{Q}} + \frac{\partial\mathscr{Q}'}{\partial\mathscr{P}'}\frac{\partial\mathscr{P}'}{\partial\mathscr{Q}} & \frac{\partial\mathscr{Q}'}{\partial\mathscr{P}'}\frac{\partial\mathscr{P}'}{\partial\mathscr{P}} \\ \frac{\partial\mathscr{P}'}{\partial\mathscr{Q}} & \frac{\partial\mathscr{P}'}{\partial\mathscr{P}} \end{pmatrix}, \tag{14}$$

at the return points (l_q, l_p). This gives

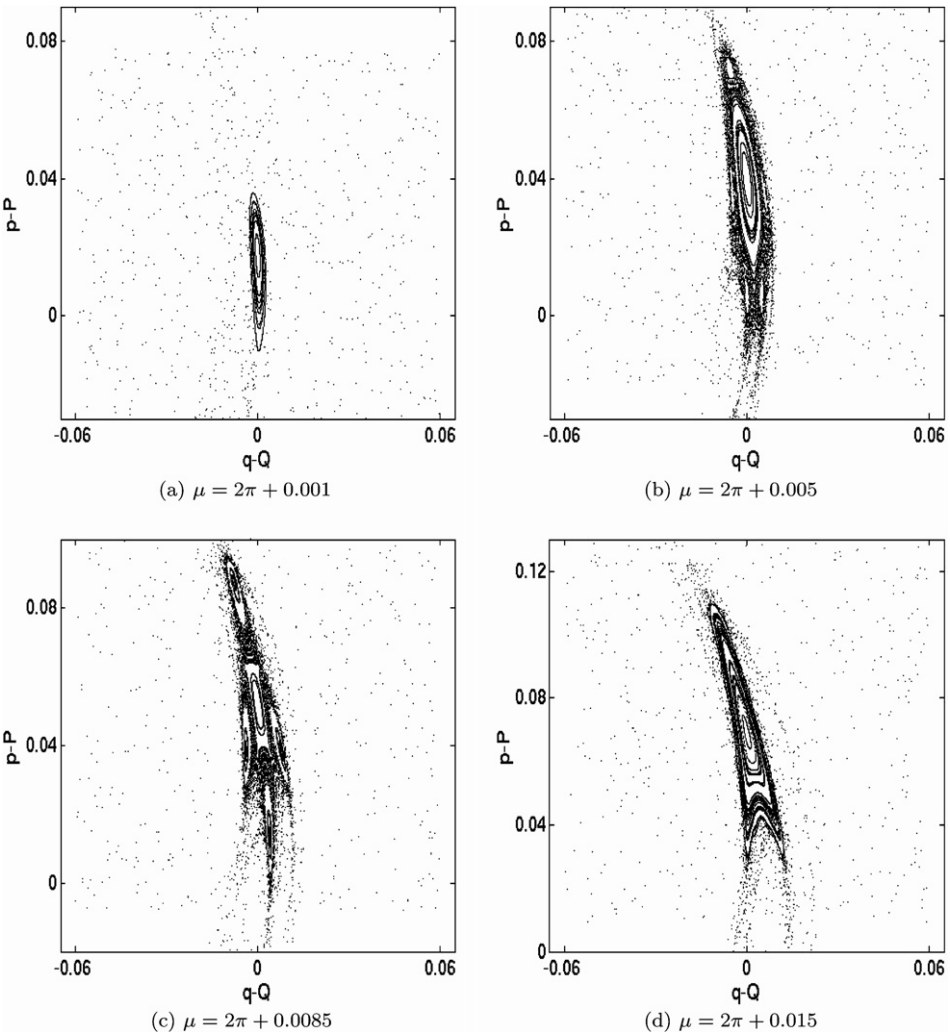

Fig. 4. Graphs showing structure of a $+\hat{\imath}$ ballistic channel for various values of the kicking strength μ and with $(n_q, n_p) = (4, 3)$. These graphs are generated by operating with the map (12) on a randomly distributed ensemble of initial phase space points.

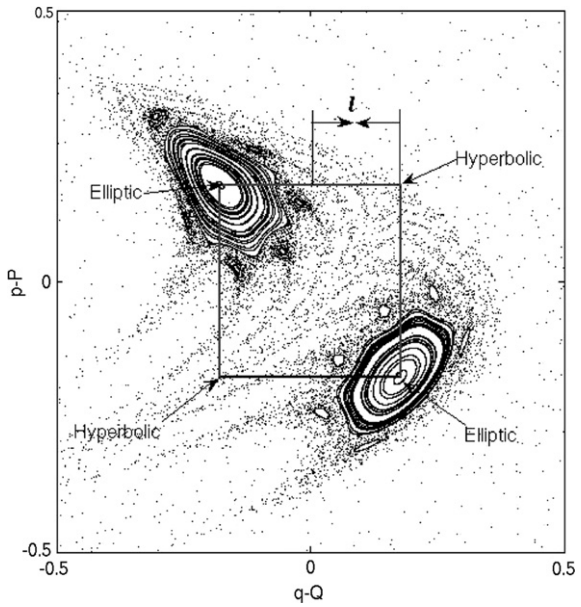

Fig. 5. The diagonal ballistic channels consist of 4 return points, 2 stable and 2 unstable. The exact location of the return points is give by the square in the diagram above. It has a length of side of $2l$ where $l = \cos^{-1}(2\pi/\mu) \approx 0.17724$ with $\mu = 2\pi + 0.1$.

$$\mathbf{J} = \begin{pmatrix} 1 + \mu^2 \sin(l_q)\sin(l_p) & \mu \sin(l_p) \\ \mu \sin(l_q) & 1 \end{pmatrix}. \tag{15}$$

Making the substitution $\overline{p} = \mu \sin(l_p)$ and $\overline{q} = \mu \sin(l_q)$ we may write $\mathbf{J}$ as

$$\mathbf{J} = \begin{pmatrix} 1 + \overline{q}\overline{p} & \overline{p} \\ \overline{q} & 1 \end{pmatrix}. \tag{16}$$

The eigenvalues of the Jacobian $\mathbf{J}$ determine if a point is stable or unstable [22]. Complex conjugate eigenvalues on the unit circle $\lambda_{1,2} = e^{\pm i\sigma}$ correspond to elliptic and therefore stable orbits. Real reciprocal eigenvalues $\lambda_2 = \lambda_1^{-1}$ correspond to hyperbolic periodic orbit and therefore the existence of unstable manifolds. The eigenvalues of this Jacobian matrix are

$$\lambda_{1,2} = \frac{1}{2}(2 + \overline{q}\overline{p} \pm \sqrt{4\overline{q}\overline{p} + \overline{q}^2\overline{p}^2}). \tag{17}$$

These eigenvalues are always real if $\overline{q}$ and $\overline{p}$ have the same sign and complex if the signs of $\overline{q}$ and $\overline{p}$ are different and their absolute values are less than *2*. The condition for the existence of the elliptic points is therefore

$$|\overline{q}| = |\overline{p}| = |\mu \sin(l)| = |\mu \sin(\cos^{-1}(2m\pi/\mu))| < 2. \tag{18}$$

Remembering that the periodic points only occur when $\mu \geqslant 2m\pi$ and noting that $\sin(\cos^{-1}(2m\pi/\mu) = \sqrt{\mu^2 - (2m\pi)^2}/\mu$ we can see that the map only has stable return points when μ is in the range

$$2m\pi < \mu < \sqrt{(2m\pi)^2 + 4}. \tag{19}$$

This compares nicely the stability condition for accelerator modes in the standard map or kicked rotor [23,24]. In that model the stability condition is $2m\pi < \mu < \sqrt{(2m\pi)^2 + 16}$.

To numerically check our value for $m = 1$ we choose starting points $(\mathscr{Q}, \mathscr{P}) = (\pm l + 0.0000001, \mp l + 0.0000001)$, where $l = \cos^{-1}\left(\frac{2\pi}{\mu}\right)$ and evolve the map (11) over *128* discrete timesteps. The phase points should circle the stable return points until we approach this special value of μ. This is exactly what we see in Fig. 6.

Following a similar procedure for the maps (12) and (13) gives us two return points at $(0, \pm l)$ or $(\pm l, 0)$ respectively, where again $l = \cos^{-1}(2m\pi/\mu)$. One of these points is always unstable while it can be shown that the other point is stable

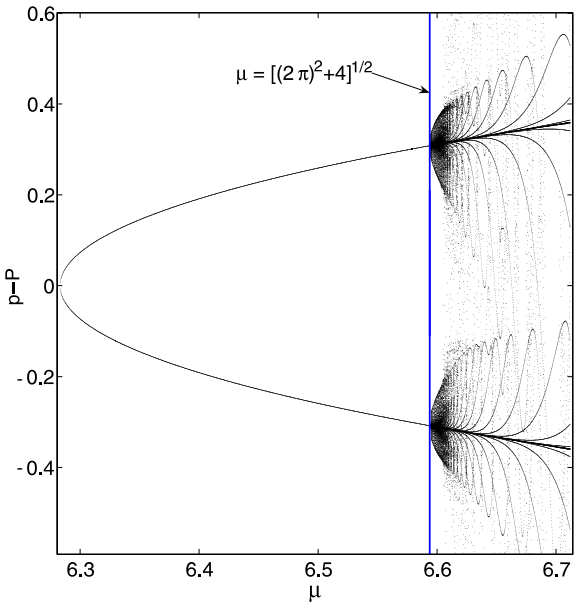

Fig. 6. Plot of $\mu - v - \mathscr{P}$ over first *128* time steps. The initial starting values $(\mathscr{Q}, \mathscr{P})$ are $(\pm\cos^{-1}(2\ \pi/\mu) + 0.0000001,\ \mp\cos^{-1}(2\pi/\mu) + 0.0000001)$. The vertical line in the graph represents where our analysis predicts the return point to become unstable. The numerical calculation shows that our analysis to be correct.

in the range $2m\pi < \mu < \sqrt{2[(m\pi)^2 + \sqrt{(m\pi)^4 + 4}]}$, see Fig. 7. We numerically check this by examining subsequent p values of a particle initially placed near the stable return point, see Fig. 8. That is at $(0, l + 0.0000001)$ and $(n_q, n_p) = (2, 1)$. Subsequent configurations only move away from the return point when $\mu > \sqrt{2[(m\pi)^2 + \sqrt{(m\pi)^4 + 4}]}$.

From the above analysis it is clear that the diagonal ballistic modes are much more significant than the vertical and horizontal modes. They are stable for a greater ranges of the perturbation μ and because each one contains two stable

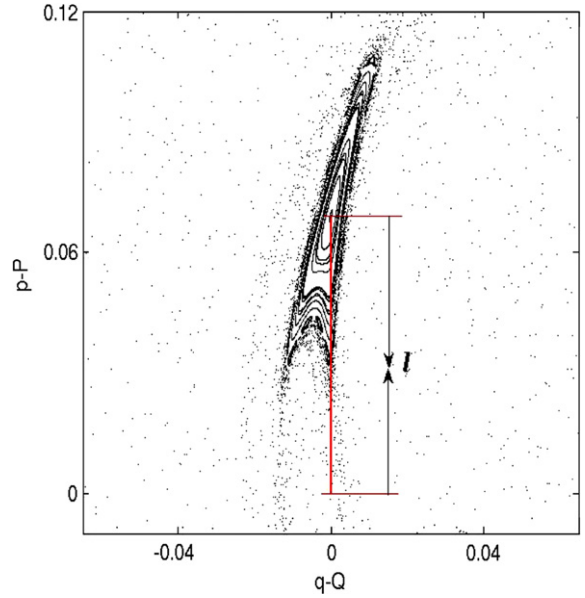

Fig. 7. The centre of this stable $-i$ horizontal channel is located at $(Q, P) = (0, l)$ where in this case $\mu = 2\pi + .015$ so that $l = \cos^{-1}(2\pi/\mu) \approx 0.069$.

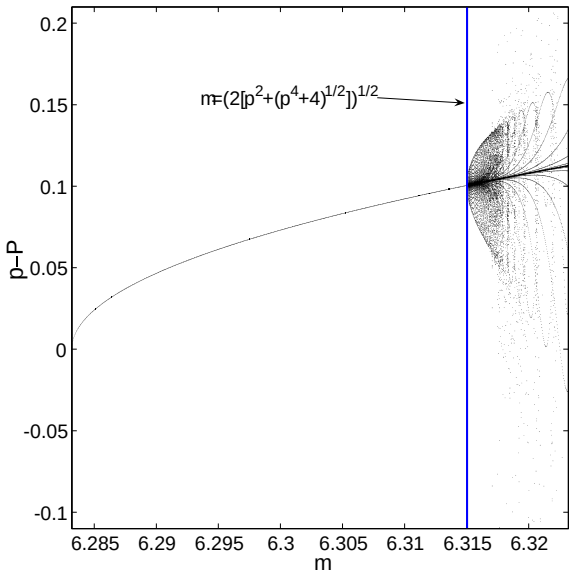

Fig. 8. Plot of $\mu - v - \mathscr{P}$ over first *128* time steps. The initial starting values $(\mathscr{Q}, \mathscr{P})$ are $(0, \cos^{-1}(2\,\pi/\mu) + 0.0000001)$. In this example $(Q, P) = (2\pi, 3\pi/2)$ The vertical line in the graph represents where our analysis predicts the elliptical stable point to become unstable. Again the numerical calculation shows our analysis to be correct.

islands they are always larger. In addition, because points on these islands move diagonally in phase space, their increase in energy over one iteration is, on average, twice that of their vertical and horizontal counterparts.

5. Conclusion

This completes our analysis of the accelerator modes. We have shown how the idea of primary trajectories can be used to derive a new mapping on which linear stability analysis becomes straight forward. The exact locations of the modes are now known and the ranges of kick parameter for which they are stable are calculated explicitly. Knowledge of this underlying classical structure is essential for proper analysis of the quantum accelerator modes to be possible. This article will act as a suitable starting point for such an analysis.

Acknowledgement

This research was supported by funding from Enterprise Ireland under the research grant EI SC/2001/059.

References

[1] Zaslavsky GM, Zakharov MYu, Sagdeev RZ, Usikov DA, Chernikov AA. Sov Phys JETP 1986;64:294.
[2] Chernikov AA, Sagdeev RZ, Zaslavsky GM. Physica D 1988;33:65.
[3] Lichtenberg AJ, Wood BP. Phys Rev A 1989;39:2153.
[4] Zaslavsky GM, Sagdeev RZ, Usikov DA, Chernikov AA. Weak Chaos and Quasi-Regular Patterns. New York: Cambridge University Press; 1991.
[5] Dana I, Amit M. Phys Rev E 1995;51:R2731.
[6] Kolmogorov AN. Dokl Akad Nauk SSSR 1954;98:527.
[7] Arnol'd VI. Russ Math Survey 1963;18:9;
Arnol'd VI. Russ Math Survey 1963;18:85.
[8] Moser J. Nachr Akad Wiss Gottingen II, Math Phys Kd 1968;1:1.
[9] Fromhold TM et al. Phys Rev Lett 2001;87:046803.
[10] Fromhold TM et al. Nature 2004;428:726.

[11] Gardiner SA, Cirac JI, Zoller P. Phys Rev Lett 1997;79:4720.
[12] Harper PG. Proc Phys Soc 1955;A68:874.
[13] Zaslavsky GM, Zakharov MYu, Sagdeev RZ, Usikov DA, Chernikov AA. Sov Phys JETP 1986;44:451.
[14] Afanasiev VV, Chernikov AA, Sagdeev RZ, Zaslavsky GM. Phys Lett A 1990;144:229.
[15] Zaslavsky GM, Sagdeev RZ, Usikov DA, Chernikov AA. Minimal chaos, stochastic webs, and structures of quasi-crystal symmetry. Sov Phys Usp 1988;31:887.
[16] Zaslavsky GM, Niyazov BA. Fractional Kinetics and accelerator modes. Phys Rep 1997;283:73.
[17] Zaslavsky GM. Chaos, fractional kinetics and anomalous transport. Phys. Rep. 2002;371:461.
[18] Kells GA. Quantum Chaos and the delta kicked harmonic oscillator 2005, PhD dissertation.
[19] Daly MV. Classical and Quantum chaos in a non-linearly kicked harmonic oscillator, 1994; PhD Thesis.
[20] Daly MV, Heffernan DM. Chaos in a resonantly kicked oscillator. J Phys A: Math Gen 1995;28:2515.
[21] Daly MV, Heffernan DM. Dynamically enhanced chaotic transport. Chaos, Solitons & Fractals 1997;8:933.
[22] Lichtenberg AJ, Lieberman MA. Regular and chaotic dynamics. 2nd ed. New York: Springer-Verlag; 1992.
[23] Ichikawa YH, Kamimura T, Hatori T. Stochastic diffusion in the standard map. Physica D 1987;29:247.
[24] Ishizaki R, Horita R, Kobayashi T, Mori H. Anomalous diffusion due to accelerator modes in the standard map. Prog Theo Phys 1991;85:1013.